JP1.10 AEROSOL-CLOUD-RADIATION AND SURFACE FLUX INTERATIONS SIMULATED IN A LARGE-EDDY MODEL

Hongli Jiang [1,2] and Graham Feingold[2]
[1]NOAA Earth Systems Research Laboratory/CIRA, 325 Broadway, Boulder, Colorado
[2]NOAA Earth Systems Research Laboratory, 325 Broadway, Boulder, Colorado

1. INTRODUCTION

Aerosol-cloud interactions are often modelled as relatively simple systems, either in parcel models with prescribed dynamics or in dynamical models that usually include only microphysical-dynamical feedbacks. However the potential exists for numerous other feedbacks via aerosol-radiative heating and surface forcing. For example, continental, convective clouds are driven by surface heating. The presence of aerosol reduces the net surface radiation (particularly if the aerosol has an absorbing component). The balance between net surface radiation and the sum of sensible and latent heat fluxes implies a reduction in these surface fluxes, and reduced convection. It is therefore important to consider aerosol-cloud interactions in this coupled system.

We present large eddy simulations that study aerosol-cloud-radiation and surface flux interactions in a warm cumulus cloud regime over land (Jiang and Feingold, 2006). There we showed that when only microphysical-dynamical feedbacks are considered (i.e., aerosol is treated only as cloud condensation nuclei, CCN), an increase in aerosol concentrations results in an increase in droplet number concentrations and reduction in precipitation, while LWP and cloud fraction remain relatively unchanged. When aerosol radiative properties are included, the reduction in net surface radiation leads to a reduction in surface sensible and latent heat fluxes, and results in significant reduction in cloud fraction and LWP. Selected results from Jiang and Feingold (2006) are presented here. Readers are referred to the paper for further details and references therein.
[1]

2. MODEL AND CASE DESCRIPTION

The model is a large eddy model based on the Regional Atmospheric Modeling System (RAMS, version 4.3, Cotton et al., 2003) coupled to a microphysical model described by Feingold et al., (2005). For a detailed description of the various elements of the model, readers are referred to Jiang and Feingold (2006). The model includes coupling between microphysics, dynamics, aerosol, radiation and a land surface model. Aerosol and drops are size-resolved and prognostic equations are solved for each bin. Aerosol radiative properties are calculated for particles that are partially absorbing (single scattering albedo of 0.9 at ~ 500 nm), with calculations dependent on ambient relative humidity. Simulations are based on a sounding on 26 September, 2002 at 7:38 LT (11:38 UTC) from a continental site in Brazil (Fazenda) during the Smoke Aerosols, Clouds, Rainfall and Climate (SMOCC) experiment (Andreae et al. 2004). The simulations are performed for 500 min. The domain size is 6.4 km x 6.4 km x 5 km with $\Delta x = \Delta y = 100$ m and $\Delta z = 50$ m. The time step is 2 s. Two sets of three-dimensional simulations were performed, as summarized in Table 1. Set 1 (S1) treats the aerosol as cloud condensation nuclei CCN only, to study aerosol-cloud interactions without radiation and surface feedbacks. Set 2 (S2) also includes the direct coupling of aerosol heating with the dynamical model and the land surface model.

Table 1. Description of Simulations. N_a is aerosol concentration; τ_a aerosol optical depth (dry); $\tau_{a,rh}$ is optical depth associated with the hydrated aerosol on the initial RH profile.

EXP	N_a cm^{-3}	τ_a	$\tau_{a,rh}$	Aerosol heating
S1-100	100	0.04	0.05	No
S1-500	500	0.20	0.26	No
S1-1000	1000	0.40	0.53	No
S1-2000	2000	0.80	1.05	No
S2-100	100			Yes
S2-500	500			Yes
S2-1000	1000			Yes
S2-2000	2000			Yes

3. SIMULATION RESULTS

3.1 *Time series*

Figure 1 shows time series of the various fields for S1 simulations. LWP (averaged only over columns that have LWP > 20 g m^{-2}) shows

[1] *Corresponding author address:* Hongli Jiang, NOAA/ESRL/CIRA, Boulder, CO 80305; e-mail: Hongli.Jiang@noaa.gov

no clear dependence on N_a over the range 100 $cm^{-3} < N_a < 2000$ cm^{-3} although the increase in aerosol does change the frequency and duration of cloud events. It has a number of distinct maxima that are correlated with higher cloud fraction (Fig. 1b), a deeper cloud layer (Fig. 1c), and surface drizzle event (Fig. 1d). Surface drizzle events occur only when clouds grow deep enough (~700 m), LWP exceeds about 400 g m^{-2}, and then only for the cleaner cases (N_a = 100, 500 cm^{-3}). Surface rain is suppressed for the polluted cases (N_a = 2000 cm^{-3}) because of a reduction in the growth of drops via collision coalescence. The increase in N_a results in higher $N_{d,int}$ (vertically integrated number concentration of droplets).

Figure 2 shows a similar plot as in Fig. 1 except for S2 simulations. LWP, cloud fraction, and cloud depth show distinct decreases with increasing aerosol amounts (Fig. 2a-c), particularly when comparing results for clean (N_a = 100 cm^{-3}) and polluted (N_a = 2000 cm^{-3}) cases. Precipitation is now suppressed at N_a > 500 cm^{-3}. The domain-maximum $w'w'$ (averaged over the horizontal plane), a measure of the strength of convection, is plotted since $N_{d,int}$ variability is similar to that in S1. Fig. 2f shows total surface heat flux ($F_{sen+lat}$, the sum of the surface sensible and latent heat fluxes). It is seen that the increase in N_a tends to decrease convective activity and surface fluxes.

3.2 *S1 and S2 Comparisons*

A sample of fields presented in Fig.1 and 2 are now time-averaged over the last 5 h (11 h to 16 h LT) and plotted as a function of N_a (Fig. 3). The general tendencies with respect to increases in N_a are quite different in S2 from those in S1.

In the S1 simulations, as N_a increases from 100 cm^{-3} to 2000 cm^{-3}, strong correlations between N_a, N_d, and τ_c are clear (Fig. 3c,e) even though LWP is not necessarily constant (Fig. 3a). The effect of increasing N_a on the net radiative flux (Fig. 3g) and the heat flux at the surface is small (Fig. 3h), in spite of the doubling in τ_c from clean to polluted cases, because of the small cloud fractions. There is a great deal of dynamical variability in all the fields at any given N_a (not shown for S1 for clarity).

The results for the S1 simulations show some subtle but important differences from the hypothesis that an increase in N_d (number concentration of droplets) results in clouds with higher LWP and cloud fraction as a consequence of reduced precipitation (the second indirect effect, e.g. Albrecht, 1989). Although some weak trends appear to be due to aerosol, the dynamical variability in LWP and cloud fraction at any given N_a is much greater than the aerosol-induced change in LWP. The suppression of precipitation does not lead to a distinct increase in LWP if all drop sizes are included in the LWP calculation (Fig. 3a). There is even some suggestion of a decrease in cloud fraction with increasing N_a which runs counter to the accepted hypothesis, possibly due to the fact that under polluted conditions, the more numerous, smaller droplets evaporate more efficiently (Xue and Feingold, 2006).

In S2, when N_a increases from 100 cm^{-3} to 2000 cm^{-3}, the cloud-averaged LWP decreases by 64% (Fig. 3a); cloud fraction decreases by 58% (Fig. 3b); and cloud depth decreases by 62% (Fig. 3d) (all calculations relative to S2-100), although there is still a great deal of dynamical variability at any given N_a . The increase in N_a leads to a smaller increase in the vertically integrated $N_{d,int}$ than in S1 due to reduced convective activity associated with the suppressed surface fluxes (Fig. 2f). The smaller increase in $N_{d,int}$ and larger decrease in LWP result in an increase in cloud optical depth from S2-100 to S2-500, and then a decrease back to roughly the same value as S2-100. The clouds become optically thinner above N_a = 500 cm^{-3}, largely because of the decreasing cloud depth and LWP. The solid square in Fig. 3a shows that LWP does increase with increasing N_a when the precipitating drops (r > 25 μm) are removed from the LWP calculations.

Decreases in R_{net} (Fig. 3g) relative to S1 range from 8% for the clean (S2-100) to a maximum of 31% for the polluted (S2-2000) case. The commensurate reduction in the surface total heat flux (Fig. 3h) leads to a maximum of 1.32 ^{o}C surface cooling relative to the S1 simulation for the most polluted conditions (Fig. 3f).
For S2 simulations, there are two competing factors at work: first, convective activity tends to increase with increasing N_a as stabilization due to precipitation progressively diminishes; second, convective activity decreases with increasing N_a as surface fluxes are reduced. On average, the cleaner clouds do tend to be characterized by stronger convection.

4. SUMMARY

4.1 *Simulations with no aerosol-radiative-land surface feedbacks*

- Increases in N_a in these warm cumulus clouds do not lead to statistically significant changes in cloud fraction, LWP and cloud depth. Aerosol effects are well within the dynamical variability in LWP and cloud fraction at any given N_a.

- Increases in N_a result in increases in N_d and cloud optical depth τ_c.

- Increases in N_a cause reduction in surface precipitation.

4.2 *Simulations including aerosol-radiative-land surface feedbacks:*

- The radiatively-active aerosol blocks up to 26.5 % of incoming solar radiative flux from reaching the surface (for the most polluted case). The reduction in the surface radiative flux leads to a reduction in the surface heat flux and consequently weaker convection, much shallower clouds and lower cloud cover and LWP.

- Cloud optical depth shows non-monotonic behavior with increasing aerosol.

We have shown that the sign of the change of aerosol induced effects on LWP and cloud fraction does not follow the common hypothesis known as the second aerosol indirect effect. This study has pointed to the importance of coupling aerosol radiative properties and a surface soil and vegetation model to the microphysical-dynamical model. As shown here, under polluted conditions the surface flux response to the aerosol may be the single most important factor in cloud reduction. We emphasize that further study is required to establish the robustness of these results for different atmospheric soundings.

ACKNOWLEGEMENTS: This work was supported by NOAA's Climate Goal and NASA's IDS and Radiation programs.

4.3 References

Albrecht, B. A., (1989). Aerosols, cloud microphysics, and fractional cloudiness, *Science*, 245, 1227—1230.

Andreae, M. O., Rosenfeld, D., Artaxo, P., Costa, A. A., Frank, G. P., Longo, K. M., Silva-Dias, M. A. F, (2004). Smoking rain clouds over the Amazon. *Science*, 303, 1337-1342.

Cotton, W. R., R. A. Pielke Sr., R. L. Walko, G.E. Liston, C.J. Tremback, H. Jiang, R.L. McAnelly, J.Y. Harrington, M.E. Nicholls, G.G. Carrio, and J. P. McFadden, (2003). RAMS 2001: Current status and future directions. *Meteorol. Atmos. Phys*., doi: 10.1007/s00703-001-0584-9.

Feingold, G., H. Jiang, and J. Y. Harrington, (2005). On smoke suppression of clouds in Amazonia, *Geophys. Res. Lett.* 32, L02804, 10.1029/2004GL021369.

Jiang, H. and G. Feingold, (2006). Effect of aerosol on warm convective clouds: Aerosol-cloud-surface flux feedbacks in a new coupled large eddy model. *J. ophys. Res*. 111, D01202, doi:10.1029/2005JD006138.

Xue, H. and G. Feingold, (2006). Large eddy simulations of trade wind cumuli: Investigation of aerosol indirect effect. *J. Atmos. Sci, in press.*

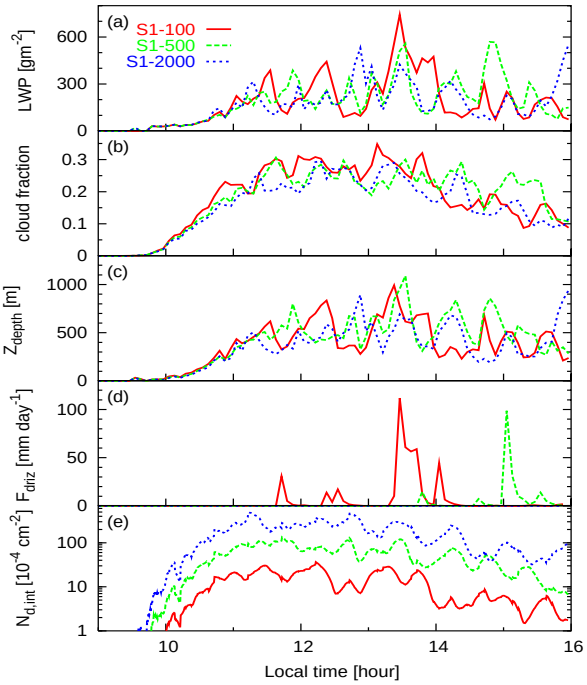

Figure 1. Time series of (a) LWP, (b) cloud fraction, (c) cloud layer depth, (d) surface drizzle rate, and (e) vertically integrated number concentration of droplets for S1 simulations.

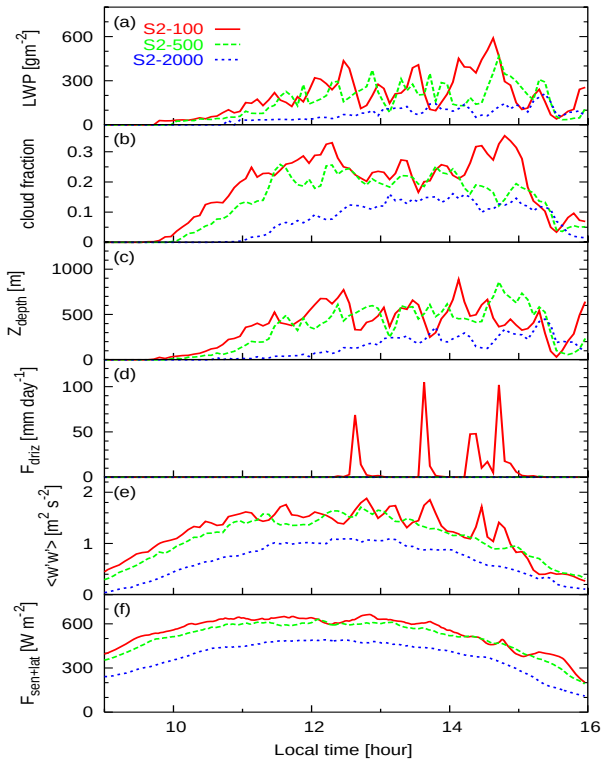

Figure 2. As in Fig. 1, but for time series of S2 simulations; (e) maximum domain average <*w'w'*> which is a measure of convective activity. (f) sum of sensible and latent heat fluxes.

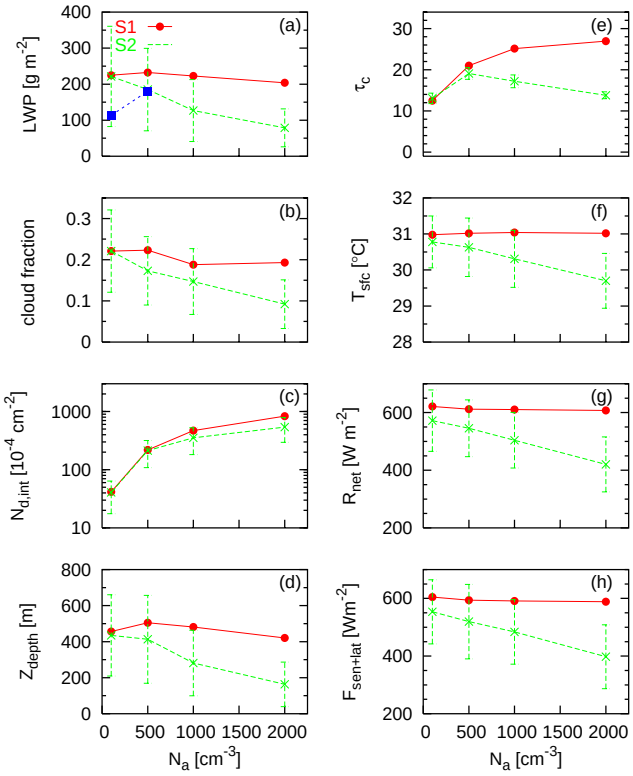

Fig. 3. Variables are time averaged over the last 5h shown in Fig. 1 and 2 for both S1 and S2 simulations. Vertical lines represent the standard deviation for S2. (a) LWP averaged over cloudy columns. The solid squares in Fig. 3a are calculations of the LWP for cloud droplets with radius <25 μm. (e) Cloud optical depth, (f) surface temperature, (g) net surface radiation, and (h) sum of sensible and latent heat fluxes. S1 results (without standard deviations) are superimposed for comparison.